Wood Sci. Technol. 17:259–277 (1983)

Wood Science and Technology

Dynamic Sorption and Hygroexpansion of Wood Wafers Exposed to Sinusoidally Varying Humidity *

A. Chomcharn

Royal Forest Department, Bangkok, Thailand

C. Skaar

Department of Forest Products, Virginia Polytechnic Institute and State University, Blacksburg, USA

Summary. Round wood wafers, 4 mm thick along the grain and 2 cm in cross-sectional diameter, of green basswood (*Tilia americana* L.), yellow birch (*Betula alleghaniensis* Britton), and black cherry (*Prunus serotina* Ehrh.), and initially dried to equilibrium in air of 77% relative humidity and 25 °C, were exposed to sinusoidally varying relative humidity between 77 and 47% at 25 °C for many cycles at each of four different cycling periods, 5.33, 10.67, 16.0 and 25.33 hours. Moisture changes and radial and tangential dimensional changes in response to the imposed humidities, measured during initial drying and subsequent cycling, gave the following results:

1. The moisture and dimensional changes were generally sinusoidal but lagged behind the imposed humidity. The phase lag decreased and the amplitude increased with increasing cycling period. Both responses and phase lags approached repetitive or "steady-state" values as cycling was prolonged.

2. A numerical solution for moisture diffusion, assuming a constant diffusion coefficient and sinusoidally varying boundary moisture conditions, was used to simulate the average moisture content in the wafer at any time. The resulting curves were qualitatively similar to those obtained experimentally, the differences attributed primarily to the effects of hysteresis and stress relaxation.

3. The mean moisture diffusion coefficients, calculated from steady-state phase lag data combined with an analytical solution of the diffusion equation, decreased with increasing cycling period. The values obtained increased with decreasing wood specific gravity as anticipated, but their magnitudes were somewhat lower than theoretical values.

4. The dynamic moisture expansion coefficient was relatively constant during successive cycles, with no consistent effect of cycling period. The dynamic values were generally higher than the static values.

5. The dynamic humidity expansion coefficient increased with increasing cycling period. It was only about half that obtained from static experiments, presumably because of hysteresis.

6. The dynamic moisture sorption coefficient, which is the effective slope of the dynamic sorption isotherm, decreased with increasing number of cycles and decreasing cycling period. It was less than half the calculated static sorption isotherm in the same humidity range, presumably due to hysteresis.

* This paper is based on a PhD. dissertation of the senior author in the Wood Products Engineering Department of the SUNY College of Environmental Science and Forestry, Syracuse, NY 13210, USA. The authors are indebted to Dr. C. H. de Zeeuw for his contribution to the dissertation as co-advisor

Introduction

Wood products in service are normally exposed to continuous cyclical changes of the environment. Daily and seasonal variations of temperature and humidity cause the moisture content of wood in service to change. This, in turn, results in dimensional changes whose magnitude depends on many factors, such as the inherent characteristics of species, history, dimensions, and duration of exposure, as well as on protective treatments applied to the products.

Numerous studies on shrinking and swelling of wood have been conducted. Information obtained from those studies alone, however, is not sufficient to predict the dimensional stability of wood in service. For example, basswood, as pointed out by Panshin and de Zeeuw (1980), exhibits very high initial shrinkage from the green to ovendry conditions. Nevertheless, it undergoes relatively small changes in dimensions with moisture changes after its initial drying, and is quite suitable for general use. Sorption studies, which express the functional relationship between equilibrium moisture content and relative humidity, have emphasized theories, mechanisms, and controlling factors.

The purpose of this study, therefore, is to investigate the interrelationships among moisture sorption, dimensional changes, time, and relative humidity. Since relative humidity is the single most important external factor governing the physical properties of wood, the emphasis was placed on measuring the moisture and dimensional responses of wood to cyclically varying relative humidity.

Review of Literature

A general review of moisture sorption and the accompanying dimensional changes has been given in the first paper in this series (Chomcharn et al. 1983). The present review will be confined to sorption and hygroexpansion under cyclic environmental conditions.

The term "movement" has been applied to dimensional changes that take place when wood which has already been dried is subjected to changes in atmospheric humidity conditions (Handbook of Hardwoods 1956, 1972; Harris 1961; Stevens 1963; Panshin, de Zeeuw 1980). The Handbook of Hardwoods (1956, 1972) suggests the following procedure for evaluating the comparative movement of different wood species which have already been kiln dried. They are successively conditioned in air at 90% RH and then at 60% RH, both at 77 °F. The EMC at these two RH conditions, together with the corresponding tangential and radial dimensional changes, are determined as percentages of the dimensions at 90% humidity. The sums of the radial and tangential movements thus calculated are used to classify each wood as having small (less than 3.0%), medium (3.0 to 4.5%), or large (greater than 4.5%) movements.

Harris (1961) exposed New Zealand hardwoods and softwoods as well as some exotic softwoods to equilibrium with three consecutive humidity cycles between 65% and 95% relative humidity, all at 26 °C. At the beginning and end of each 24 hour cycle, moisture contents and tangential dimensions were determined. At the end of the last cycle, total swelling was determined by soaking the samples in

water. Moisture content increases and tangential swellings after 24 hours at 95% RH were compared among species to indicate the short term relative dimensional stability. Total swelling and shrinkage intersection points, obtained from another set of samples were used as a basis for judging the long term dimensional stability of those species. He pointed out that the practical applications of results depend on the type of exposure to which timber was subjected. Where periodical wetting or prolonged exposure to alternatively high and low humidities is probable, standard shrinkage or swelling figures are applicable. For exposure to short term fluctuations in atmospheric humidity, the rate of movement is more important.

Studies of the swelling and shrinkage of wood subjected to cyclic moisture changes under external mechanical restraint have received special attention in recent years in connection with the rheological behavior of wood, particularly creep. Although creep and deformation of wood under restraint are beyond the scope of this study, some of the methods used and results obtained from those studies carry implications for the present investigation and therefore will be mentioned briefly.

Perkitny (1960) studied the deformation behavior of pine sapwood samples restrained by clamps and subjected to cyclic soaking and drying for 18 cycles. A similar study was conducted by Bolton et al. (1974) in which initially ovendry samples, clamped under radial restraint, were subjected to 10 cycles of water soaking and oven-drying. Armstrong and Kingston (1962) studied the effect of cyclic moisture content changes on creep in wood under bending, compressive, and tensile stresses. Bryan and Schniewind (1965) noted that the moduli of rupture and of elasticity of particleboard, cycled between 20% and 6% EMC for 7 days at each condition, decreased with increase in number of cycles, and creep progressively increased. Wilkinson (1966) observed that end-connected Douglas-fir beams deformed one to 6.5 times more under load when subjected to three 14-day cycles between 95% RH (90 °F) and 45% RH (160 °F) than when maintained at 50% RH (74 °F).

Schniewind (1967), and Schniewind and Lyon (1973) studied the creep-rupture life of Douglas-fir beams, as functions of varying environmental conditions. It was found that square wave humidity cycling had a more severe effect than sinusoidal cycling on the creep-rupture life of beams. Cycled beams failed at much shorter times than those maintained at uniform conditions. Temperature cycling was of only minor importance except for its indirect effect on moisture content changes. The integral moisture change appeared to be the most important factor in determining creep-rupture life under cyclic conditions. This factor in turn depended on the size of beam and length of the cycling period.

Narayanamurti and Verma (1972), Tokumoto (1973), and Takahashi and Schniewind (1974) have reported on studies of swelling and deformation of wood under conditions of mechanical restraint and cyclic moisture changes.

Experimental Procedures

The same chamber and measurement instruments used for the initial drying experiment described previously (Chomcharn et al. 1983) was employed in this part of

the study. The dewpoint temperature control used a thermistor as the sensing element in one active arm of a bridge (Fig. 1). The adjacent active arm consisted of a step-variable resistance such that the water temperature was programmed to vary in discrete steps according to a predetermined schedule. There were a total of 48 discrete steps for each complete humidity cycle, each step corresponding to 360/48 or 7.5 degrees. Thus, the relative humidity inside the test chamber varied sinusoidally with time between 47 and 77% (± 1.5%). The dry bulb temperature controller was replaced by a thermistor controller for convenience in regulation and was kept constant at 25 ± 0.25 °C. The relative humidity was controlled between the limits of 47 to 77 ± 1.5%. Dimensional changes could be sensed to ± 125 microinches (± 3 μm) and weight changes to ± 0.5 mg.

The same samples used for the initial drying were also used in this portion of the study. After each sample attained equilibrium at 25 °C and 77% relative humidity, the cyclic tests began. This involved recording of the dimensional and moisture responses of the wood to sinusoidally varying relative humidity. Since cycling was started at the peak value, the relative humidity generated was in fact a cosine function. Four different cycling frequencies were arbitrarily chosen as dictated by the timing generator available. These gave cycling periods T_0 of 5.33, 10.67, 16.00, and 26.67 hours, corresponding to the time ratios 1 : 2 : 3 : 5, respectively. Each set of test samples within a species was exposed to only one cycling period. Basswood samples were subjected only to the longest and shortest cycling periods. The same parameters recorded during the initial drying (sample weight, radial and tangential dimensions, dry bulb temperature, wet-bulb depression and water bath or dewpoint temperature) were also recorded during the cycling experiments.

Repeated cycling of relative humidity was carried out until the response amplitudes of the dimensional and weight changes became stable, as indicated by peak values of successive cycles attaining constant values (Fig. 2). Cycling was always stopped at the lowest humidity (47%), and samples were allowed to equilibrate at this condition for approximately 12 hours before the experiment was

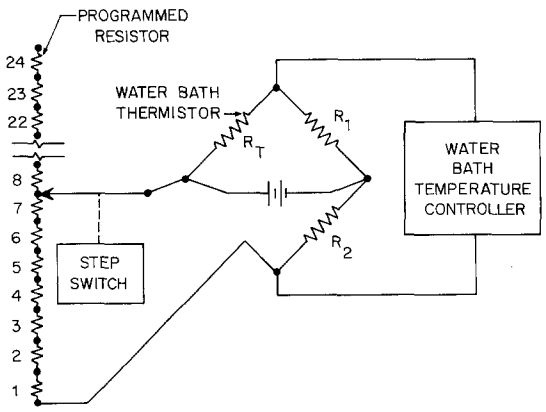

Fig. 1. Schematic diagram of circuit used to program and control the dewpoint water bath temperature

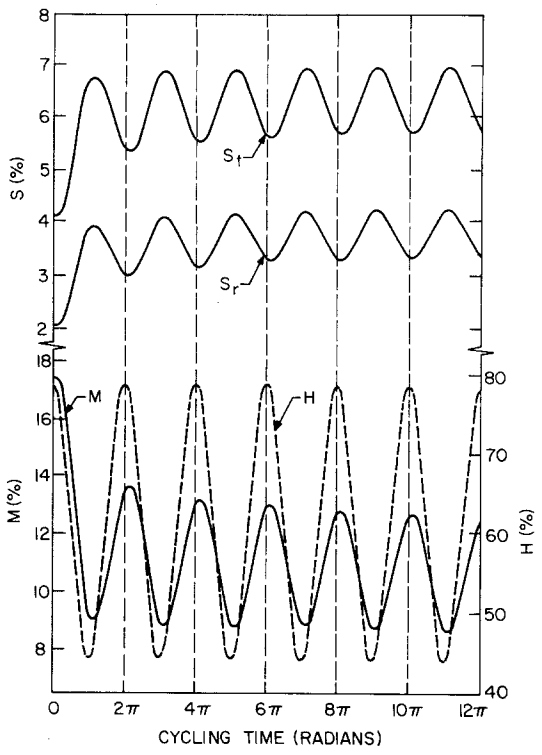

Fig. 2. Plots of humidity (H), moisture content (M) and tangential (S_t) and radial (S_r) shrinkages against cycling time, in radians, for birch cycled at T_0 of 26.67 hours

terminated. Samples were then weighed and dimensions measured, after which they were oven dried at 103 ± 2 °C for final determination of moisture content.

The same procedures reported in the first part of this series (Chomcharn et al. 1983) were used to reduce the data plotted on the multipoint recorder into digital form for computer analysis of the results, that is, each parameter was digitized at fifteen minute real time intervals.

Diffusion Equations Used

The process involved in unsteady state moisture diffusion in wood is usually described in terms of Fick's second law which relates the change in concentration C (g/cm^3) at any location (cm) in a sample per unit of time t (seconds) to the diffusion coefficient D (cm^2/s). It can be written in approximate form in terms of moisture content M, for the case of a constant coefficient D, and for one-dimensional movement, as

$$\partial M/\partial t = D(\partial^2 M/\partial x^2). \quad (1)$$

For the present case, the solution of Eq. (1) for a sinusoidally varying boundary condition is desired.

Equation (1) can be written in terms of dimensionless variables E, Υ and X in place of the variables M, t and x, giving (Crank 1956),

$$\partial E/\partial \Upsilon = \partial^2 E/\partial X^2 . \quad (2)$$

Here $E=[M-\bar{M}_e]/[(M_e)_{max}-\bar{M}_e]$, $(M_e)_{max}$ being the equilibrium moisture content of the cycling air corresponding to the highest humidity H_{max} used in the cycle (77% in this case), $\bar{M}_e$ the *mean* of $(M_e)_{max}$ and $(M_e)_{min}$, the minimum value for M_e of the air ($H_{min}=47\%$ in this case); $\Upsilon = tD/a^2$ and $X=x/a$, the fractional distance from $x=0$ at the center of the sample to $x=\pm a$ at the two surfaces, the total sample thickness being 2a. The maximum and minimum possible values for E therefore are ± 1.

Two general methods for solving Eqs. (1) or (2) were used in this study. Both of these assume that D and a are constant, and neither account for factors such as moisture sorption hysteresis, stresses associated with moisture gradients, or time-dependent stress relaxation effects.

The first solution discussed here is by a numerical method, the Schmidt method in particular. This is followed by consideration of two analytical solutions.

Schmidt Numerical Solution

The principle involved in the Schmidt numerical method is described by Crank (1956). A variation of it has been used by Simpson (1974) for analyzing the dependence of D for wood on its moisture content. In the present case, D is taken to be constant.

In the numerical method used here, the sample of half-thickness a, drying from both surfaces ($x=\pm a$) is divided into small finite increments, each of thickness δx, or of fractional thickness δX. Likewise, time t or Υ is divided into small finite increments δt or $\delta\Upsilon$. In the Schmidt method, the numerical form of Eqs. (1) or (2) are simplified by maintaining the relationship

$$\delta\Upsilon = (1/2)\,(\delta X)^2 \quad (3)$$

which reduces Eq. (2) for example to

$$E_m^+ = (1/2)\,(E_{m+1}+E_{m-1}) \quad (4)$$

where the subscript m refers to the m^{th} increment of δX, and the superscript + refers to an additional increment in $\delta\Upsilon$. In other words, E_m is the value of E at the location $m\delta X$ in the sample at time Υ, and E_m^+ is the value of E_m at $\Upsilon+\delta\Upsilon$. Similarly, the values E_{m+1} and E_{m-1} are the values of E at time Υ and locations $(m+1)\,\delta X$ and $(m-1)\,\delta X$, respectively. Equation (4) states that E_m^+, that is E at location $m\delta X$ and at time $\Upsilon+\delta\Upsilon$ is equal to the mean value of E at locations on both sides of location m at time Υ.

The results obtained by Eq. (4) approach those of Eq. (2) as $\delta\Upsilon$ and δX become vanishingly small. In this study, δX was taken as 0.1; and, therefore, $\delta\Upsilon$, by Eq. (3) was 0.005. For the present work, the mean value $\bar{E}$ of E_m throughout the sample was desired. This was obtained by numerical integration using the trapezoidal rule for each increment, δX, for each value of Υ.

The variation of $\bar{E}$ with time depends on the initial conditions in the sample and also on how the surface conditions vary with time. To simulate the present experiments, the initial value of E in the sample is uniform and equal to +1. The surface condition E_s is assumed to vary with time t as a cosine function between +1 and −1. Thus,

$$E_s = \cos(2\pi\, t/T_0) = \cos(2\pi\, \Upsilon/\Upsilon_0) = \cos(2\pi\, N) \tag{5}$$

where $\Upsilon_0 = T_0 D/a^2$ and $\Upsilon/\Upsilon_0 = N$ the number of cycles. The variation of E_s with Υ is in discrete steps when Υ is replaced by $n\delta\Upsilon$ and Eq. (5) becomes

$$E_s = \cos(2\pi\, n\, \delta\Upsilon/\Upsilon_0) = \cos(2\pi n/n_0) = \cos(2\pi\, N) \tag{6}$$

where n is the number of increments of $\delta\Upsilon$ and $n_0\,(=\Upsilon_0/\delta\Upsilon)$ is the number of increments in one complete cycle. Thus $n/n_0 = \Upsilon/\Upsilon_0$. The ratio $\delta\Upsilon/\Upsilon_0$ (or $\delta\Upsilon/T_0$) should be sufficiently small (less than 0.01) so that the cosine function is simulated within reasonable limits. One of the constraints in the Schmidt method is that $\delta\Upsilon = (1/2)(\delta x)^2$ (Eq. 3).

Analytical Solutions

The numerical solution of the diffusion equation is useful for predicting the general moisture response characteristics of wood samples subjected to sinusoidally varying humidity. However, analytical solutions are also available for the "steady-state" case that is when the response is repetitive in succeeding cycles. Two of these are discussed here.

Carslaw and Jaeger (1959) give a solution for the diffusion of heat through a slab of thickness 2 a subjected to sinusoidally varying temperatures at both surfaces. In terms of moisture diffusion, their solution for the steady-state condition can be written

$$E(X, \Upsilon) = A\cos[(2\pi\, \Upsilon/\Upsilon_0) + \varphi] \tag{7}$$

where A and φ are functions of X but independent of Υ. The functions A and φ given by Carslaw and Jaeger can be written in the form,

$$A = [(\cos(2\,KX) + \cosh(2\,KX))/(\cos(2\,K) + \cosh(2\,K))]^{1/2} \tag{8a}$$

$$\varphi = \arctan[\tan(KX)\cdot\tanh(KX)] - \arctan[\tan(K)\cdot\tanh(K)] \tag{8b}$$

where $K = (\pi/\Upsilon_0)^{1/2}$.

In order to obtain the mean value $\bar{E}(\Upsilon)$ in the sample at any time Υ, Eq. (7) must be integrated over the limits of X = 0 to 1 (or −1 to +1). Such an analytical integration was not available for this function so it was integrated numerically using the trapezoidal rule, with $\delta X = 0.1$.

A second analytical solution arises from the solution to an important problem in heat diffusion. This is the equation which describes the variations in temperature at various depths in the earth when the surface is subjected to harinonically varying temperature such as the daily and annual variations in surface temperatures (Carslaw, Jaeger 1959). An analogous equation applies when a wood sample of very long length is subjected at one end surface to a sinusoidally varying humidity.

The solution to the one-dimensional diffusion equation in this case can be written

$$E(Z, \Upsilon) = \exp(-KZ)\,[\cos(2\pi\,\Upsilon/\Upsilon_0) - KZ] \tag{9}$$

where Z is the distance from the surface.

For the case of a wood sample of finite thickness 2a with both surfaces exposed to cyclically varying moisture content, using the principle of reflection and superposition, Eq. (9) can be modified to

$$E(Z, \Upsilon) = \sum_{n=0}^{\infty} (-1)^n \cdot \cos[(2\pi\,\Upsilon/\Upsilon_0) - 2n\,K - KZ] \tag{10}$$
$$+ (-1)^n \cdot \exp[-(2n+2)\,K - KZ] \cdot \cos[(2\pi\,\Upsilon/\Upsilon_0) - (2n+2)\,K - KZ]$$

where $Z = 1 - X$.

Equation (10) can be integrated with respect to Z from $Z = 1$ to 0 (or for $X = 0$ to 1) to yield $\bar{E}(\Upsilon)$. Thus

$$\bar{E}(\Upsilon) = (1/K)\left\{1/2\,[\cos(2\pi\,\Upsilon/\Upsilon_0) + \sin(2\pi\,\Upsilon/\Upsilon_0)]\right. \tag{11}$$
$$\left. + \sum_{n=1}^{\infty} (-1)^n\,[\exp(-2n\,K)]\,[\cos((2\pi\,\Upsilon/\Upsilon_0) - 2n\,K) + \sin((2\pi\,\Upsilon/\Upsilon_0) - 2n\,K)]\right\}$$

Equation (11) is particularly useful for evaluating the theoretical response of the mean value $\bar{E}$ as a function of Υ for any given value of $K\,(=\pi/\Upsilon_0)^{1/2}$ since it is not necessary to integrate numerically as is the case for Eq. (7). However, it is necessary to sum the various terms for successive values of n, although the series converges rapidly, particularly for large values of K.

General Phenomenological Behavior

The general responses of all samples to sinusoidally varying humidity over several cycles were similar to those shown for yellow birch in Fig. 2. After a transient period of several cycles, the moisture and dimensional responses approach a steady-state or repetitive pattern. In order to analyze the responses of the moisture and dimensional changes to the cyclic humidity changes, a curve-fitting procedure was used, as described below.

Curve-fitting Procedure

The curve-fitting procedure was designed to fit sinusoidal curves to the observed curves of H, M, S_t and S_r for each set of samples. The dimensional changes S_t and S_r were based on the green dimensions in each case. The parameters of the curves giving the best fit were then used to compare the moisture and dimensional change responses of each sample with the relative humidity variations.

In order to compare the sample responses to the applied humidity cycles, the following equation, based on Fourier analysis, was used for fitting all of the observed curves, including the humidity curves.

$$2\,G = G_{max} + G_{min} + [G_{max} - G_{min}]\,[A_0 \sin \omega t + B_0 \cos \omega\, t] \tag{12}$$

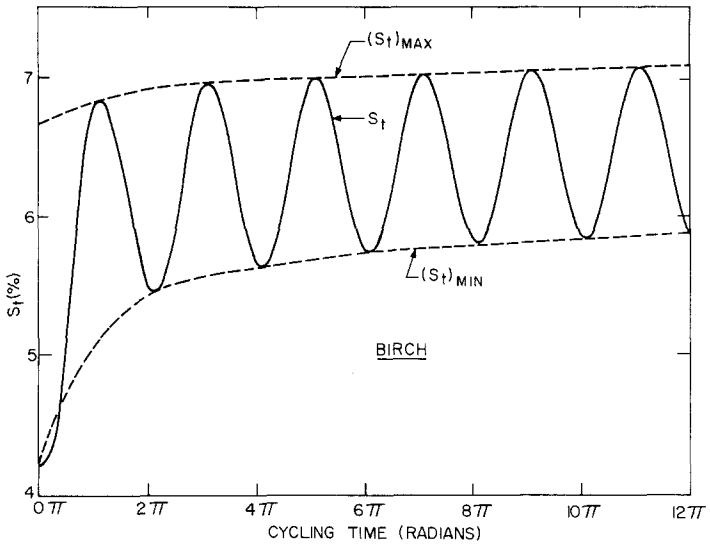

Fig. 3. Plots of tangential shrinkage (S_t) and of $(S_t)_{max}$ and $(S_t)_{min}$ against cycling time, in radians, for birch cycled at T_0 of 26.67 hours

where G is the observed value of the function (H, M, S_t or S_r). The terms G_{max} and G_{min} are the peak values of G, obtained by fitting a polynomial to the observed maximum and minimum peaks. The terms A_0 and B_0 are the Fourier coefficients for the fundamental angular frequency ω ($=2\pi/T_0$, where T_0 is the period).

Figure 3 shows the calculated curves for the maximum and minimum tangential shrinkages $(S_t)_{max}$ and $(S_t)_{min}$ for birch cycled at $T_0=26.67$ hours. These form an envelope for the observed cyclic tangential shrinkage curve also shown.

Equation (12) can be rearranged into the following form.

$$A_0 \sin \omega t + B_0 \cos \omega t = \frac{2G - G_{max} - G_{min}}{G_{max} - G_{min}} = Q \tag{13}$$

where Q is used to represent the complex expression involving the G terms. By Fourier analysis, the terms A_0 and B_0 were evaluated by the use of the approximation equations,

$$A_0 \cong (1/j) \sum_{i=1}^{j} (Q_i \sin (2\pi \Upsilon/\Upsilon_0) \cdot \delta\Upsilon) \tag{14}$$

$$B_0 \cong (1/j) \sum_{i=1}^{j} (Q_i \cos (2\pi \Upsilon/\Upsilon_0) \cdot \delta\Upsilon) \tag{15}$$

thus reducing the digitized data to obtain the constant A_0 and B_0 in each case. The term j corresponds to the number of discrete equally spaced time steps at which readings of the observed values of G were digitized for each complete cycle.

The phase angle γ (radians) was calculated for H, M, S_t and S_r for each cycle by use of the equation,

$$\gamma = \arctan (A_0/B_0). \tag{16}$$

Ideally, the phase angle γ for the humidity H should have been zero in each case. However, this was not realized because of various uncontrollable experimental factors, particularly the thermal lag involved in heating or cooling the water bath for dewpoint control. The average calculated humidity phase angle for each run ranged from 0.0035 to 0.038 radian (0.2 to 2.2 degrees). Those for the response curves of M, S_t and S_r were much larger, ranging from 0.26 to 0.94 radian (15 to 54 degrees).

The phase lag φ of each response curve (M, S_t and S_r) was calculated by subtracting the phase angle γ of each response cycle from that of the corresponding humidity cycle. The results of these calculations are discussed later.

Having calculated values of A_0 and B_0 for a given test, and the empirical polynomials for G_{max} and G_{min}, it was possible to compute and plot curves of G, obtained by use of Eq. (12), and compare these with the observed curves of G. Excluding the first cycle, the agreement was quite good in most cases with a maximum residual difference of less than one percent. The relatively large deviation (ca. 5%) in the first cycle is probably due to the difficulty in fitting equations for G_{max} and $G_{min.}$ to adequately describe the first cycle.

Observed Phase Lag Response

In all cases, there was a phase lag φ in the response of the wood samples to the sinusoidally varying humidity. The phase lag decreased with increasing number of cycles, approaching constant values as the number of cycles increased.

The moisture phase lag φ_m for a given cycle was generally greater than those for the dimensional changes φ_r and φ_t. This may be related to the fact that stresses associated with moisture gradients generally have a greater effect on dimensional than on moisture changes. There were also differences in the tangential φ_t and radial φ_r phase lags.

Figure 4 shows a plot of the average phase lag $\bar{\varphi}$ (mean of φ_m, φ_r and φ_t) against number of cycles n for each of the four cycling periods for birch. It is clear that as the cycling period T_0 increases, the phase lag decreases. This is as anticipated because with longer cycling periods the sample response more nearly follows the humidity changes. For very long cycling periods, the internal moisture contents of the sample should be essentially uniform, and equal to the equilibrium conditions at the surface.

Omitting the first cycle, the data for phase lag against cycle number N for each test was fitted to an empirical equation of the form

$$\bar{\varphi} = 1/(A + BC^N) \tag{17}$$

where A, B and C are empirical constants. From the fitted curves such as those shown in Fig. 4, as well as from Eq. (17), it is clear that $\bar{\varphi}$ decreases as N increases. becoming asymptotic to the value 1/A, since C is less than unity in all cases.

Observed Amplitude Response

Figure 5 shows how the moisture contents of birch samples responded to the cyclic humidity changes of two different periods, one (curve B) five times the other

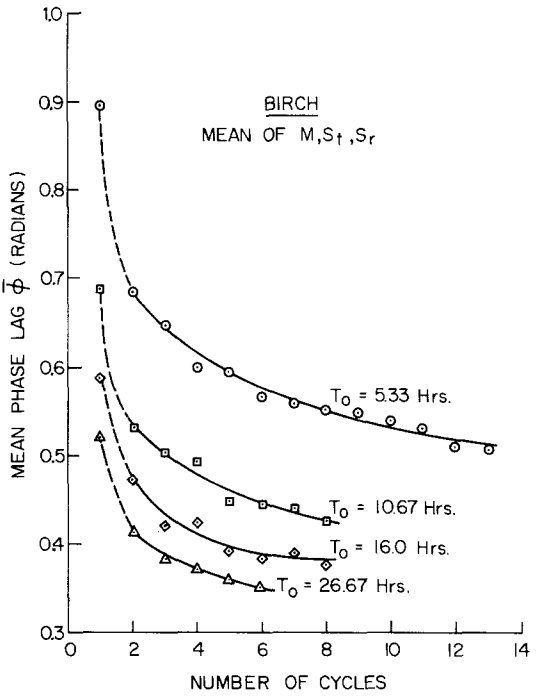

Fig. 4. Plots of mean phase lag $\bar{\varphi}$ against number of cycles for birch at each of four different cycling periods (T_0)

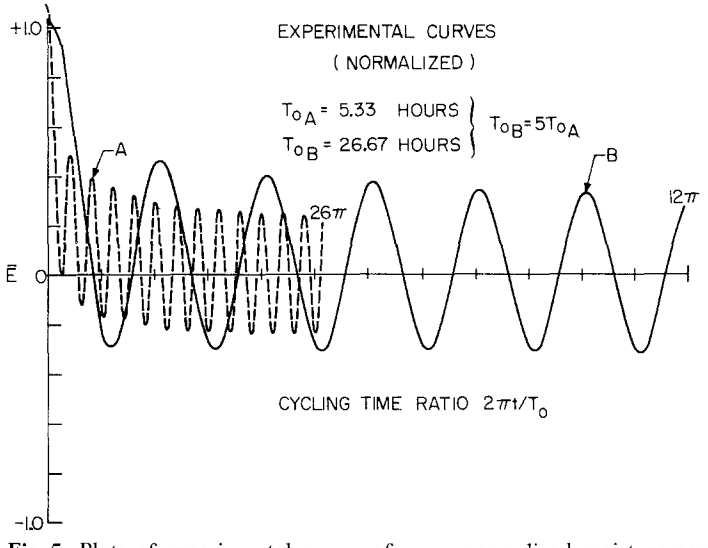

Fig. 5. Plots of experimental curves of mean normalized moisture content $\bar{E}$ against time in radians for birch with T_0 of 26.67 and 5.33 hours, a ratio of 5 : 1

(curve A). These curves were plotted in terms of $\bar{E}$, the normalized mean sample moisture content as defined in Eq. (2).

It is apparent that the amplitude decreases rapidly to a steady-state condition where the response is repetitive in subsequent cycles. The number of cycles required to attain the steady-state response is greater for the sample subjected to the shorter cycle (curve A) although the total time required is about the same in both cases. Furthermore, the response amplitude is less for the sample subjected to the shorter cycle.

It should be noted that the surface moisture content M_s fluctuations and the corresponding value of E_s were not strictly sinusoidal even though the humidity variation was sinusoidal. This is because of both hysteresis and the non-linearity of the sorption isotherm.

Comparison of Observed and Theoretical Responses

Figure 6 shows the Schmidt numerical solution given by Eq. (4) for the expected variation of $\bar{E}$ with time, of a sample subject to sinusoidally varying surface moisture content as given by Eq. (6). Two curves are shown, one of which (curve B) is the simulated solution for a cyclic period T_0, five times that of the other (curve A).

Comparing Fig. 6 with the experimental curves shown in Fig. 5, it is apparent that the same general behavior was observed as was predicted by the Schmidt solution to the diffusion equation. The response amplitude is lower in each case for the sample (curve A) subjected to the shorter period of surface humidity oscillation. Furthermore, the approach to the steady-state condition is similar in both cases.

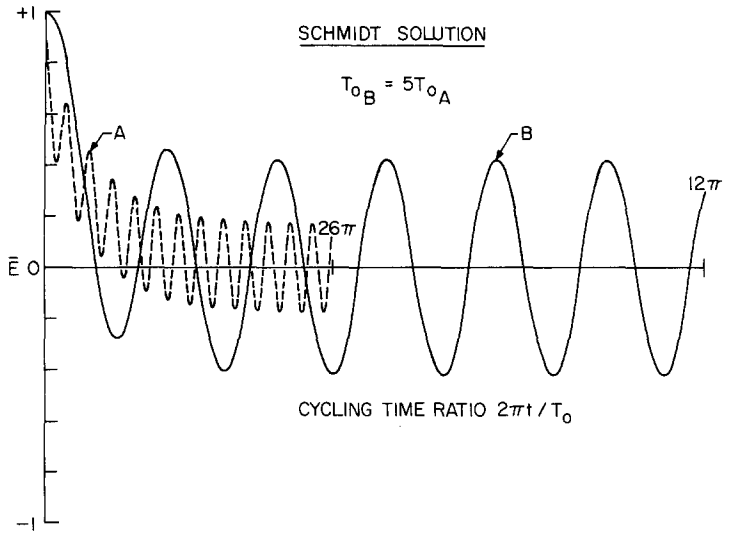

Fig. 6. Plots of Schmidt solution of mean normalized moisture content $\bar{E}$ against time in radians for two different cycling periods T_0

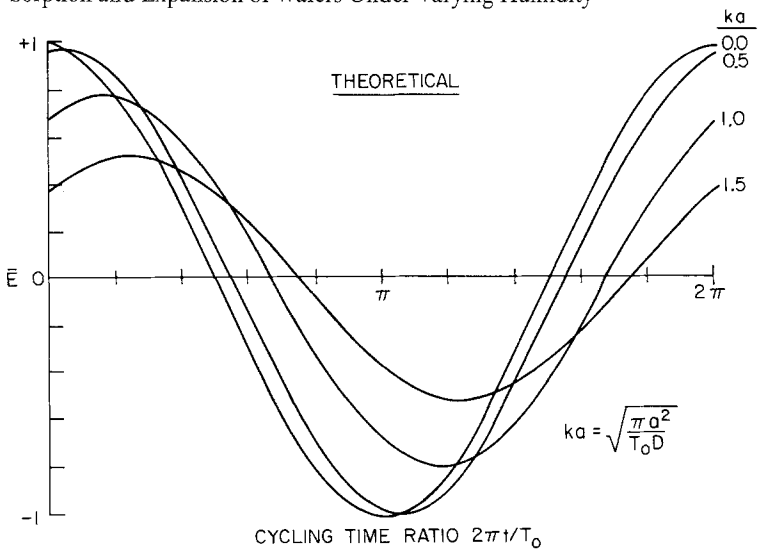

Fig. 7. Plots of theoretical steady-state normalized moisture content $\bar{E}$ against $2\pi t/T_0$ for a single period for different values of K (=ka)

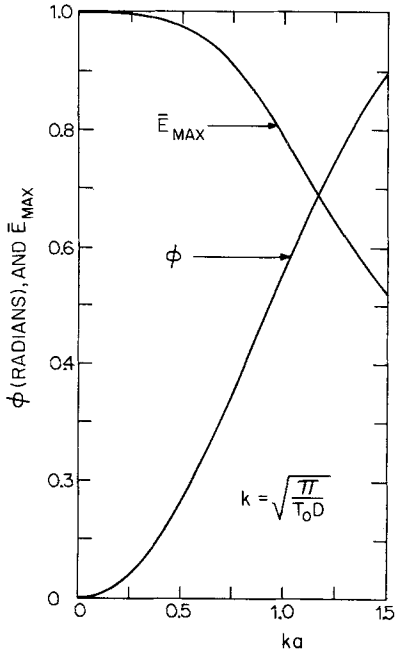

Fig. 8. Plots of theoretical values of $\bar{E}_{max}$ and φ as functions of K (=ka)

It has already been indicated (Fig. 4) that the phase lag φ of the samples as determined experimentally increased with decrease in the length of the period T_0 of the humidity cycle. This is also true for the theoretical steady-state response as is shown in Figs. 7 and 8. These also show that response amplitude decreases with increasing K (ka) or decreasing period T_0.

The curve shown in Fig. 8, which gives the theoretical relationship between the phase lag response φ and the coefficient K was fitted to an empirical equation to give

$$K = 0.2762 + 1.4015\ \varphi - 0.1173\ \varphi^2 - 0.00369\ \varphi^3 \quad (18)$$

over the range for K of 0.5 to 1.0, well within the range of experimental data. The value of K for a given sample was calculated from Eq. (18) using the mean phase lag $\bar{\varphi}$ observed during the steady-state response portion of each experiment. The phase lag φ was equivalent in each case to 1/A obtained by fitting Eq. (17) to the experimental data (Fig. 4).

Knowing K for a given sample, the apparent diffusion coefficient D was calculated by use of the relationship $K = (\pi/\Upsilon_0)^{1/2}$ defined in equations (8) and (9), and $\Upsilon_0 = T_0\ D/a^2$. Thus

$$D = \pi\ a^2/(T_0\ K^2) \quad (19)$$

where a is the sample half-thickness and T_0 is the cycling period. Table 1 shows the values of 1/A, a, T_0, K^2 and D (cm^2/s) obtained for a number of samples of birch, basswood and cherry.

The values for D shown in Table 1 are lower than those predicted by Siau (1971) for softwoods of the same densities based on a theoretical model for longitudinal flow. His model predicts a value for D near 15 to $20 \times 10^{-\lambda^6}$ cm^2/s at 25 °C and 12 percent moisture content for wood of 0.6 specific gravity. The means for the three woods studied here (Table 1) were about 1/3 to 1/2 of these values, ranging from 5 to 10×10^{-6} cm^2/s, increasing with decreasing specific gravity as anticipated.

Table 1 shows that, for a given species, the calculated diffusion coefficient D increases as T_0 decreases. This may be related to the phenomenon of stress-relaxation (Christensen, Kelsey 1959) which limits the rate of moisture change in samples subjected to slowly changing humidities. Under these conditions, the rate of moisture change in wood may be governed more by stress-relaxation processes than by the classical diffusion processes. This would tend to be the case when T_0 is

Table 1. Mean moisture diffusion coefficients and associated parameters calculated from steady-state phase lag data

Species	T_0	2a	$\Phi = 1/A$	K = ka	$D \times 10^6$	Specific* gravity (M = 12%)
	h	cm	rad.	cm/cm	cm^2/s	g/cm^3
Yellow birch	26.67	0.400	0.327	0.722	2.525	0.61
Yellow birch	16.00	0.403	0.387	0.789	3.659	0.61
Yellow birch	10.67	0.400	0.390	0.805	5.199	0.61
Yellow birch	5.33	0.404	0.484	0.748	8.183	0.61
Black cherry	16.00	0.409	0.347	0.748	4.132	0.50
Black cherry	10.67	0.411	0.314	0.705	6.987	0.50
Basswood	5.33	0.407	0.417	0.840	9.963	0.39

* Based on even-dry mass, and volume at M = 12%

Table 2. Summary of basic data on each wood, including regression equations of shrinkage against wood moisture content

Parameter	Yellow birch	Basswood	Black cherry
Specific gravity,* green volume, g/cm³	0.562±0.005	0.357±0.002	0.463±0.006
Specific gravity, o.-d. volume, g/cm³	0.664±0.005	0.423±0.003	0.544±0.005
Before cycling, H %	77.8 ±1.2	77.8 ±1.2	77.8 ±1.2
Before cycling, M_e %	18.63 ±0.53	15.71 ±1.38	19.05 ±1.10
Before cycling, S_{ts} %	4.31 ±0.41	5.30 ±0.16	7.24 ±0.25
Before cycling, S_{rs} %	2.43 ±0.19	3.35 ±0.09	2.42 ±0.24
After cycling, H %	47.7 ±0.7	47.7 ±0.7	47.7 ±0.7
After cycling, M_e %	8.31 ±0.51	6.75 ±0.41	9.09 ±0.30
After cycling, S_{ts} %	6.92 ±0.22	7.50 ±0.13	8.79 ±0.38
After cycling, S_{rs} %	4.88 ±0.21	5.42 ±0.18	3.51 ±0.17
Oven-dry, S_{ts} %	9.10 ±0.20	9.26 ±0.13	11.20 ±0.42
Oven-dry, S_{rs} %	6.91 ±0.16	6.94 ±0.14	4.66 ±0.24
Tangent. regression, S_{ts} %	9.02 −0.253M	9.16 −0.246M	10.20 −0.156M
Tangent. SIM %	35.7	37.2	65.4
Radial regression, S_{rs} %	6.85 −0.237M	6.98 −0.231M	4.50 ±0.109M
Radial SIM %	28.9	30.2	41.3

* Based on even-dry mass, and volume green

large, yielding lower apparent diffusion coefficients than for short cycling periods, as was found here. It also would account for lower overall values for D found here compared with anticipated values.

Transverse Hygroexpansion

Transverse hygroexpansion is discussed in terms of shrinkage S, based on green dimensions, in relation to moisture content M and relative humidity H. Furthermore, the hygroexpansion values obtained at various equilibrium moisture contents, designated here as static values, were different from the corresponding dynamic values obtained during sample exposures to cyclically varying humidities. The static shrinkage and hygroexpansion values are treated first in each case, followed by discussion of the dynamic values and their relation to the static values.

Table 2 lists the mean static shrinkage values S_{ts} and S_{rs} for each species at each of two equilibrium moisture contents, prior to the start of moisture cycling ($M_e \approx 18\%$), and after completion of moisture cycling ($M_e \approx 8\%$). Also listed are the intercepts and slopes of the linear regression equations relating S_{ts} and S_{rs} to M_e, calculated from the two equilibrium points for each species.

The intercepts of the regression equations are estimates of total expected shrinkage from the green to oven-dry condition. The measured values obtained by oven-drying the samples are also shown in Table 2. Agreement between corresponding pairs of values are generally written ±0.1% except for tangential shrinkage of cherry, for which the shrinkage obtained by oven-drying is 1.0% greater than is predicted by the regression equation.

Table 3. Calculated values of moisture (X) and humidity (Y) expansion coefficients, and the slope (Z) of the effective sorption isotherm, calculated as Y/X for each wood

	Yellow birch	Basswood	Black cherry
X_{ts} %/%	0.253	0.246	0.156
X_{rs} %/%	0.237	0.231	0.109
X_{td} %/%	0.294	0.339	0.261
X_{rd} %/%	0.244	0.182	0.195
Y_{ts} %/%	0.0867	0.0731	0.0515
Y_{rs} %/%	0.0814	0.0688	0.0362
Y_{td} %/%	0.0386	0.0346	0.0464
Y_{rd} %/%	0.0298	0.0255	0.0237
Z_s %/%	0.343	0.298	0.331
Z_d %/%	0.127	0.121	0.150
Z_d/Z_s (ratio)	0.37	0.41	0.45

The slopes of the regression equations give estimates of X_{ts} and X_{rs}, the static values of the tangential and radial moisture expansion coefficients, defined as dS_{ts}/dM and dS_{rs}/dM, respectively. The magnitudes of X_{ts} and X_{rs} are given in Table 3 for comparison with the corresponding dynamic values.

The relationships between the dynamic shrinkages S_{td} and S_{rd} and M during the cyclic tests were essentially linear for each test run. The dynamic values X_{td} and X_{rd} were calculated from the slopes of S_{td} and S_{rd} vs. M in each case. There were no consistent trends in X_{td} or X_{rd} with cycling period T_0,, so only the mean values are cited in Table 3.

The data in Table 3 indicate that the dynamic values X_{td} and X_{rd} are generally larger than the static values, particularly in the case of cherry where the difference is more than 50 percent. No satisfactory explanation is given for this difference. Possibly it is related to the periodic development and relaxation of stresses during the cycling process and the associated moisture gradients. In the case of cherry, it may be related to the fact that the shrinkage intersection point, SIM, that is the extrapolated value of the moisture content below which shrinkage begins, is much higher for cherry than for the other two woods. These intersection points were calculated in each case by dividing the zero intercept value of S_{ts} or S_{rs} by X_{ts} or X_{rs}, respectively, the absolute values of the slope for each regression equation. The values of SIM are included in Table 2. The reason for the extremely high SIM in the case of cherry is not known, although it may indicate development of some collapse during the initial drying. It is evident from Table 2 that the SIM is always several percent higher for tangential than for radial shrinkage in all cases. This agrees with the findings of Kelsey (1956) and others as reported in Skaar (1972).

The static values Y_{ts} and Y_{rs} of the humidity expansion coefficients were calculated in each case by dividing the differences in the respective shrinkages, S_{ts} and S_{rs}, before and after cycling (Table 2), by the difference in the mean equilibrium humidities, 77.8% and 47.7% (Table 2). The resulting values of Y_{ts} and Y_{rs} are listed in Table 3.

The dynamic values Y_{td} and Y_{rd} were calculated from the slopes of dS_{td}/dH and dS_{rd}/dH obtained from the cyclic humidity experiments. These coefficients

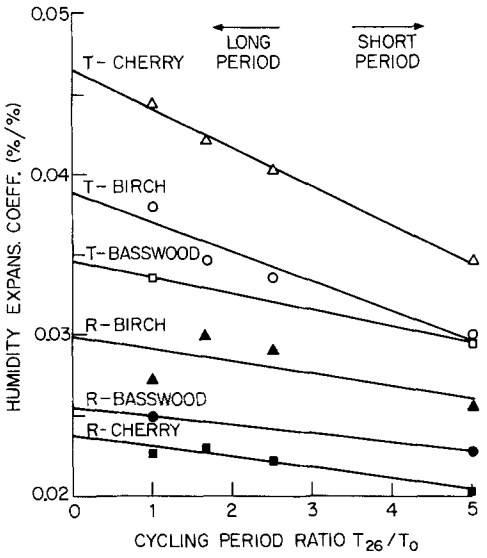

Fig. 9. Plots of dynamic humidity expansion coefficients Y_{td} and Y_{rd} against the ratio of T_{26}/T_0 for all three woods, including the regression curves in each case

increased with increase in the cyclic period T_0, as is shown in Fig. 9 where Y_{td} and Y_{rd} are plotted against the cycling period ratio T_{26}/T_0 for the three species. Table 3 lists the zero intercepts in each case. These are estimates of Y_{td} and Y_{rd} under long-term cycling conditions such as might occur during annual seasonal changes where an entire wood member cycles slowly but at nearly uniform moisture content throughout.

Comparison of the static and dynamic values of Y_t and Y_r show that the latter are generally less than half those of the static values. It is believed that this results primarily from the strong sorption hysteresis effect which greatly reduces the effective slope dM/dH of the sorption isotherm during cyclic sorption. Figure 10, which shows a plot of M against H during cyclic sorption for basswood cycled at 5.33 hours and also a portion of the static desorption and adsorption isotherms for basswood taken from Spalt (1957), illustrates this point. The slope of the long axis of the ellipse represents a mean value of dM/dH for the cyclic sorption. This is considerably lower than the slope of either the adsorption or desorption isotherms over the humidity range shown. It is recognized that this dynamic slope would be greater for a longer period T_0 but is still considerably lower than that of the static equilibrium isotherm.

The effective slope $Z = dM/dH$, of the sorption isotherm over a given humidity range, is equivalent to the ratio Y/X. The mean static value dM/dH, designated here as Z_s, over the experimental humidity range covered in this study ($H \approx 47.7$ to 77.8%), is given in Table 3 for each species. The same value is obtained for Z_s using Y_{ts}/X_{ts} or Y_{rs}/X_{rs} for a given species, because the shrinkage terms S used in calculating the corresponding X and Y terms for tangential or radial shrinkages cancel out, leaving only the M and H terms which are identical for the tangential and radial orientations.

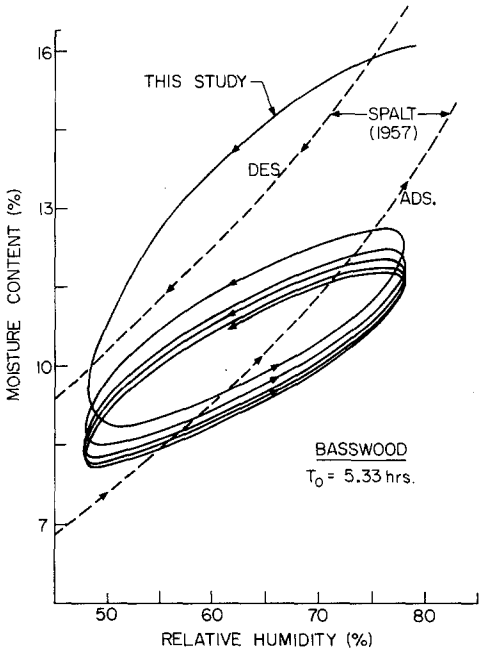

Fig. 10. Plot of moisture content (M) against relative humidity (H) for basswood cycled at 5.33 hours, together with portions of the static adsorption and desorption isotherms of basswood as given by Spalt (1957)

In contrast, the dynamic values of dM/dH, designated as Z_d, are somewhat different for Y_{td}/X_{td} and Y_{rd}/X_{rd} because the individual terms were calculated from independent measurements. However, the values obtained, while not identical, were nearly the same for a given species and only the mean values are given in Table 3.

The ratio Z_d/Z_s is also listed in Table 3 for each species. It is evident from these values that the effective slope of the dynamic sorption isotherm is only about 0.4 as great as that of the static isotherm. As mentioned previously, this is probably related to the dominance of sorption hysteresis as is indicated in the curves shown in Fig. 10. The significance of this is that calculations of moisture changes in wood due to cyclically varying humidities in service are considerably less than are predicted from the static sorption isotherms, particularly if hysteresis is neglected.

References

Armstrong, L. D.; Kingston, R. S. T. 1962: The effect of moisture content changes on the deformation of wood under stress. Aust. J. Appl. Sci. 13:257–276

Bolton, A. J.; Jardine, P.; Vine, M. H.; Walker, J. F. 1974: The swelling of wood under mechanical restraint. Holzforschung 28:138–144

Bryan, E. L.; Schniewind, A. P. 1965: Strength and rheological properties of particle boards as affected by moisture content and sorption. Forest. Prod. J. 15:143–148

Carslaw, H. S.; Jaeger, J. C. 1959: Conduction of heat in solids. 2nd ed. London: Oxford Univ. Press

Chomcharn, A. 1975: Transverse hygroexpansion of wood wafers under sinusoidally varying relative humidity. Ph.D. Thesis. SUNY Coll. Envir. Sci. and For., Syracuse, N.Y.
Chomcharn, A.; Skaar, C. 1983: Moisture and transverse dimensional changes during air-drying of small green hardwood wafers, Wood Sci. Technol. 17:227–240
Christensen, G. N.; Kelsey, K. E. 1959: The rate of sorption of water vapor by wood. Holz Roh-Werkst. 17: 178–188
Crank, J. 1956: The mathematics of diffusion. London: Oxford University Press
Handbook of Hardwoods. 1956, 1972: The handbook of hardwoods. 1st and 2nd eds. London: Her Majesty Stationary Office
Harris, J. M. 1961: The dimensional stability, shrinkage intersection point and related properties of New Zealand timbers. Tech. Paper No. 36, N.Z. For. Res. Inst., Wellington
Narayanamurti, D.; Verma, G. M. 1972: Swelling and shrinkage of wood under mechanical restraint: Influence of various factors on Tectona grandis. Holzforsch. Holzverwert. 24:83–93
Panshin, A. J.; de Zeeuw, C. 1980: Textbook of Wood Technology, 4th ed. New York: McGraw-Hill
Perkitny, T. 1960: Pressure variation in differently pre-pressed and rigidly clamped wood specimens. Holz Roh- Werkst. 18:200–210
Schniewind, A. P. 1967: Creep-rupture life of D-fir under cyclic environmental conditions. Wood Sci. Technol. 1:278–288
Schniewind, A. P.; Lyon, E. D. 1973: Further experiment of creep-rupture life under cyclic environmental conditions. Wood Fiber 4:334–341
Siau, J. F. 1971: Flow in wood. Syracuse: Syracuse Univ. Press
Simpson, W. T. 1974: Measuring dependence of diffusion coefficient of wood on moisture concentration by adsorption experiments. Wood Fiber 5:299–307
Skaar, C. 1972: Water in wood. Syracuse: Syracuse Univ. Press
Spalt, H. A. 1957: The sorption of water vapor by domestic and tropical woods. Forest. Prod. J. 7:331–335
Stevens, W. C. 1963: The transverse shrinkage of wood. Forest. Prod. J. 8:386–389
Takahashi, A.; Schniewind, A. P. 1974: [Deformation and drying set during cyclic drying and wetting under tensile loads.] J. Jpn. Wood Res. Soc. 20:9–14
Tokumoto, J. 1973: [Moisture recovery of drying set. I: Swelling behaviors of set wood. II: Effect of quantity of adsorbed moisture and dry-wet cyclings on set recovery in wood.] J. Jpn. Wood Res. Soc. 19:577–584, and 585–591
Wilkinson, T. L. 1966: Moisture cycling of trussed rafter joints. U.S. For. Serv. Res. Pap. FPL-67. Madison, Wisconsin
Wood Handbook 1974: Wood as an engineering material. Agriculture Handbook No. 72. Washington, D.C.: U.S. Government Printing Office

(Received July 13, 1982)

A. Chomcharn, Ph. D.
Royal Forest Department,
Bangkok, Thailand

C. Skaar, Prof. of Wood Physics
Department of Forest Products,
Virginia Polytechnic Institute and State University
Blacksburgh, VA. 24061, USA